The Rho guanine nucleotide exchange factor PLEKHG1 is activated by interaction with and phosphorylation by Src family kinase member FYN

Shun Nakano[1,‡], Masashi Nishikawa[1,‡], Tomoyo Kobayashi[2,‡], Eka Wahyuni Harlin[3], Takuya Ito[3], Katsuya Sato[4], Tsuyoshi Sugiyama[5] , Hisashi Yamakawa[6], Takahiro Nagase[6], and Hiroshi Ueda[1,3,*]

From the [1]United Graduate School of Drug Discovery and Medical Information Sciences, [2]Faculty of Engineering, and [3]Graduate School of Natural Science and Technology, Gifu University, Gifu, Japan; [4]Department of Molecular Pathobiochemistry, Gifu University Graduate School of Medicine, Gifu, Japan; [5]Faculty of Pharmacy, Gifu University of Medical Science, Kani, Gifu, Japan; [6]Kazusa DNA Research Institute, Chiba, Japan

Edited by Henrik Dohlman

Rho family small GTPases (Rho) regulate various cell motility processes by spatiotemporally controlling the actin cytoskeleton. Some Rho-specific guanine nucleotide exchange factors (RhoGEFs) are regulated *via* tyrosine phosphorylation by Src family tyrosine kinase (SFK). We also previously reported that PLEKHG2, a RhoGEF for the GTPases Rac1 and Cdc42, is tyrosine-phosphorylated by SRC. However, the details of the mechanisms by which SFK regulates RhoGEFs are not well understood. In this study, we found for the first time that PLEKHG1, which has very high homology to the Dbl and pleckstrin homology domains of PLEKHG2, activates Cdc42 following activation by FYN, a member of the SFK family. We also show that this activation of PLEKHG1 by FYN requires interaction between these two proteins and FYN-induced tyrosine phosphorylation of PLEKHG1. We also found that the region containing the Src homology 3 and Src homology 2 domains of FYN is required for this interaction. Finally, we demonstrated that tyrosine phosphorylation of Tyr-720 and Tyr-801 in PLEKHG1 is important for the activation of PLEKHG1. These results suggest that FYN is a regulator of PLEKHG1 and may regulate cell morphology through Rho signaling *via* the interaction with and tyrosine phosphorylation of PLEKHG1.

Rho family small GTPases (Rho) spatiotemporally regulate various cellular responses such as cell morphogenesis, proliferation, and differentiation through actin cytoskeletal rearrangement (1–3). As with other GTP-binding proteins, Rho including RhoA, Rac, and Cdc42 oscillate between an inactive GDP-bound state and an active GTP-bound state. Rho are activated by Rho-specific guanine nucleotide exchange factors (RhoGEFs), which activate Rho by promoting the conversion of GDP to GTP. On the other hand, Rho are suppressed by intrinsic GTPase activity, which is stimulated by Rho-specific GTPase-activating proteins (RhoGAPs) (1–3). In this way,

RhoGEFs and RhoGAPs play a crucial role in controlling the regulation of Rho. A major subgroup of RhoGEFs are the diffuse B-cell lymphoma (Dbl) family RhoGEFs, members of which contain a highly conserved Dbl-homology (DH) domain that catalyzes the GDP/GTP exchange, and a pleckstrin homology (PH) domain followed by a DH domain. More than 60 different Dbl family RhoGEFs have been identified in mammalian genomes (1–3). It is known that RhoGEFs are spatiotemporally regulated by various extracellular signals through an intramolecular multifunctional domain in RhoGEF.

Several RhoGEFs, including Asef and β-Pix, have been shown to be regulated through tyrosine phosphorylation by Src-family tyrosine kinases (SFKs). Asef is phosphorylated at Tyr-94 and activates Rac in a manner dependent on SFKs in epidermal growth factor (EGF)-stimulated A431 cells (4). There is a report that the phosphorylation–dephosphorylation cycle of β-Pix at Tyr-442 can serve as a key regulatory signal for focal complex assembly–disassembly in Src-transformed cells (5). Moreover, it has been reported that the phosphorylation of Tyr-2622 in TRIO is essential for the regulation of the DCC/TRIO signaling complex in cortical neurons during netrin-1-mediated axon outgrowth (6). Recently, we reported that the phosphorylation of Tyr-479 and Tyr-660 on DBS leads to actin cytoskeletal reorganization by EPHB2/SRC signaling. Based on these reports, it is thought that SFKs play an important role in RhoGEF activation (7).

SFKs are nonreceptor tyrosine kinases that are well known as oncogenic molecules. At least eight SFK members are expressed in mammals: SRC, YES, FYN, LYN, LCK, HCK, FGR, and BLK (8). Some family members, including c-Src, Yes, and Fyn, are ubiquitously expressed, while others show more restricted patterns of expression (9). It is thought that SFKs interact with various molecules in the cell and regulate several biological processes involving Rho signaling-regulated actin cytoskeletal reorganization (10). SFKs are made up of an N-terminal Src homology (SH) 4 domain that contains lipid modification sites and a poorly conserved unique domain, an SH3 domain that recognizes and interacts with proline-rich

---

sequences, an SH2 domain that recognizes and interacts with specific sites of tyrosine phosphorylation, and an SH1 tyrosine kinase catalytic domain (10, 11). SFKs tyrosine-phosphorylate target proteins and transduce a signal downstream through interaction between the phosphorylated tyrosine and a protein having the SH2 domain and thereby regulate various cellular functions. It has been reported that Src tyrosine-phosphorylates Cortactin, which controls actin polymerization, and transmits signals to the Rho family to form an actin skeletal system that originates in focal adhesions (12). Several of these SH3 domain-containing Dbl-family RhoGEFs, such as Kalirin, also contain a proline-rich region, indicating that intramolecular interactions between an SH3 domain and a polyproline region have a role in the autoinhibition of Dbl-family RhoGEFs (13). It is thought that the relationship between RhoGEFs and these functional domains of SFKs is important in oncogenic transformation.

We reported that pleckstrin homology domain-containing family G member 2 (PLEKHG2) was phosphorylated at Tyr-489 by SRC and interacted with phosphoinositide-3 kinase regulatory subunit 3 (PIK3R3) and ABL1 in a manner dependent on its tyrosine phosphorylation and later showed that the interaction between PLEKHG2 and ABL1 suppresses cell growth through intracellular protein accumulation *via* the NF-κB signaling pathway (14, 15). In general, both the DH and PH domains are responsible for GEF activity. In particular, the DH-PH domains of PLEKHG1 and PLEKHG2 share 54% identity in their amino acid sequences. There are several reports that PLEKHG1 is associated with various pathological and physiological functions in humans (16–19). It has been reported that PLEKHG1 is one of the RhoGEFs involved in the cyclic stretch-induced reorientation of vascular endothelial cells (20). In the same paper, PLEKHG1 was shown to be one of the RhoGEFs that activate Rac and Cdc42, while a later study reported that PLEKHG1 is one of the RhoGEFs that activate Cdc42 (20, 21). However, the details of the regulation of PLEKHG1 within cells, including the involvement of SFKs, are not known.

In this study, we showed that PLEKHG1 is activated through its interaction with FYN, one of the SFKs. We further showed that the enhancement of PLEKHG1 activity and the interaction between PLEKHG1 and FYN are dependent on the phosphorylation of Tyr-618, Tyr-720, and Tyr-801 in PLEKHG1.

Results

FYN, a member of SFKs, activates PLEKHG1 through its interaction with PLEKHG1 and tyrosine phosphorylation of PLEKHG1

To examine whether the signals from SFKs influence PLEKHG1 activity in the cell, we measured the level of PLEKHG1-induced SRF-dependent gene transcription, which is known to be induced by Rho family activation (22). The level of PLEKHG1-induced SRF-dependent gene transcription was enhanced in HEK293 cells coexpressing Myc-epitope tagged wild-type (WT) PLEKHG1 (Myc-PLEKHG1WT) and

Flag-epitope tagged WT FYN (Flag-FYNWT) as compared with that in cells expressing PLEKHG1WT alone or cells coexpressing other Flag-epitope tagged WT SFKs (Flag-SRCWT, Flag-YES1WT, Flag-LCKWT, and Flag-LYNWT) (Fig. 1A). Next, to investigate the level of tyrosine phosphorylation of PLEKHG1 in cells coexpressing each SFK and PLEKHG1, we analyzed the level of tyrosine phosphorylation of PLEKHG1 immunoprecipitated with anti-Myc epitope antibody in cells coexpressing each Flag-SFK and Myc-PLEKHG1. The results showed that PLEKHG1 was tyrosine-phosphorylated by coexpression with any of the SFKs and was especially strongly phosphorylated by coexpression with Flag-FYNWT. The mobility of the band of Myc-PLEKHG1 in the lysate of cells coexpressing Myc-PLEKHG1 and Flag-FYN was slower than that of cells expressing Myc-PLEKHG1 (*top* panels in Fig. 1B). In contrast, the bands of Myc-PLEKHG1 were partially shifted in the lysate of cells coexpressing Myc-PLEKHG1 and other Flag-SFKs (SRK, YES1, LCK, and LYN). The phosphorylated band intensity of PLEKHG1 was consistent with the band shift (*top* and *middle* panels in Fig. 1B), suggesting that Myc-PLEKHG1 is more strongly phosphorylated by Flag-FYNWT than the other Flag-SFKs. In addition, when we analyzed the coprecipitation of each SFK and PLEKHG1 in the same sample, Flag-FYNWT was strongly coprecipitated (Fig. 1B). Our data demonstrated that tyrosine phosphorylation of PLEKHG1 by FYN and the interaction found only with FYN may be related to the activation of PLEKHG1 by FYN.

To examine how the activation of PLEKHG1 by FYN influences the intracellular localization of PLEKHG1 and the cell morphology, we transfected HEK293 cells with an Azami-Green (mAG)-fused PLEKHG1 and/or FLAG-SFK-coding plasmid. We then performed immunofluorescent staining and fluorescent phalloidin staining and visualized cells using a confocal laser scanning microscope. First, we transfected Flag-SRC or Flag-FYN alone into HEK293 cells, and we confirmed that these kinases themselves have little effect on cell morphology (Fig. 1C). Next, we checked the effect of PLEKHG1 on cell morphological change. Consistent with the fact that PLEKHG1 is one of the RhoGEFs, most of PLEKHG1 was localized near the plasma membrane, and filopodia-like protrusions of filamentous actin were observed in cells expressing mAG-PLEKHG1WT alone (*left* panels in Fig. 1D, *arrowheads*). In addition, cells coexpressing mAG-PLEKHG1 and Flag-SRCWT showed filopodia-like protrusions with the same morphology as cells expressing mAG-PLEKHG1 alone (*middle* panel in Fig. 1D, *arrowheads*). On the other hand, PLEKHG1 was localized to lamellipodia-like actin-rich protrusions (*right* panels in Fig. 1D, *arrows*) in addition to the filopodia-like protrusions (*right* panels in Fig. 1D, *arrowheads*) in cells coexpressing mAG-PLEKHG1 and Flag-FYNWT. Next, we investigated PLEKHG1 activity toward Cdc42 in cells expressing PLEKHG1 and/or SFKs by measuring the amounts of GTP-bound Cdc42 (active Cdc42) using the GST-tagged CRIB domain of PAK1 (GST-CRIB). The strength of the amount of intracellular GTP-bound Cdc42 obtained by this method may be indirectly reflected in the guanine
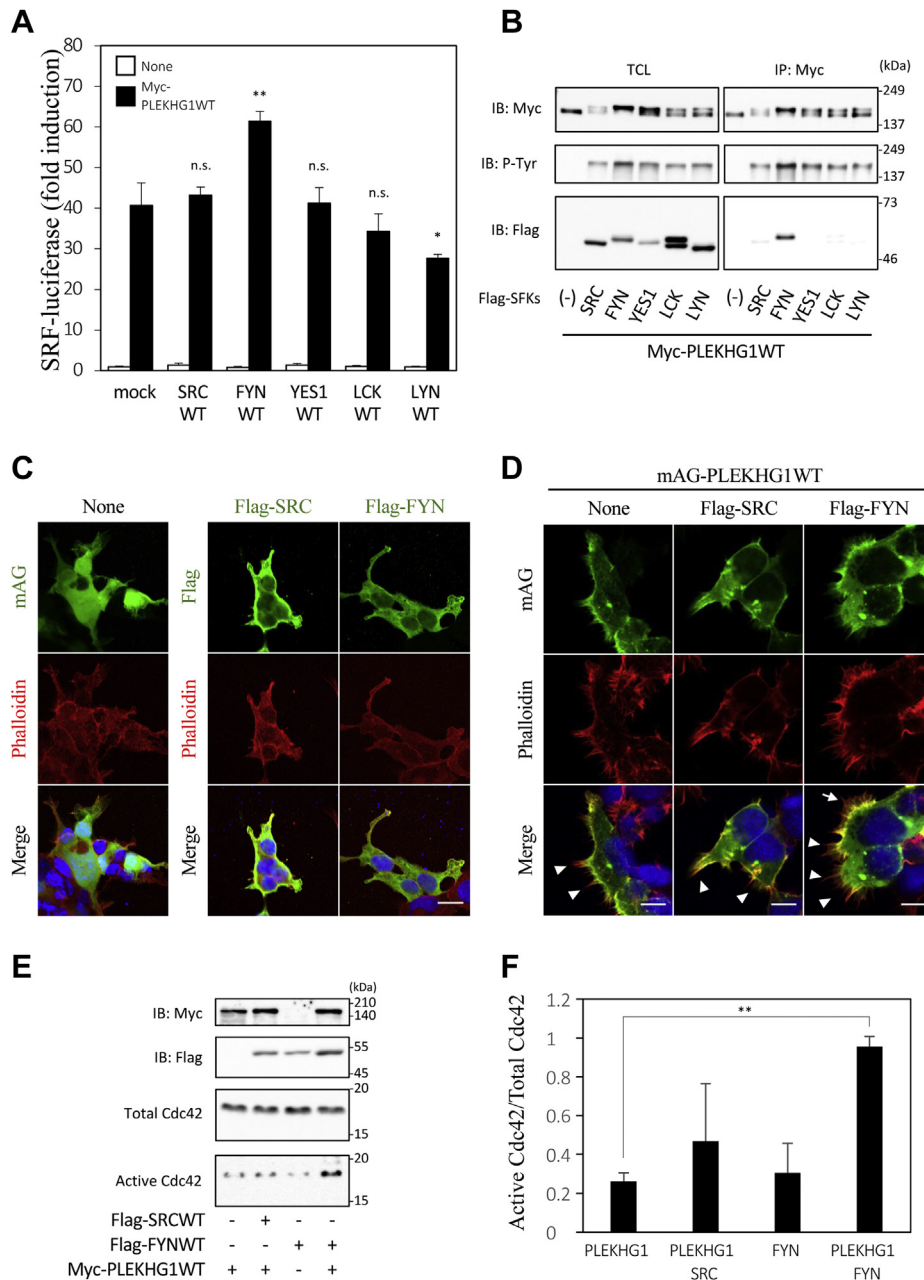
Figure 1. Signaling of FYN activates PLEKHG1 and affects PLEKHG1-induced actin cytoskeleton rearrangement in HEK293 cells. *A*, HEK293 cells were cotransfected with pSRF.L-luciferase, pRL-SV40, and expression vectors for Myc-PLEKHG1 and Flag-SRCWT, Flag-FYNWT, Flag-YESWT, Flag-LCKWT, or Flag-LYNWT, as indicated. Transfected cells were lysed 24 h after transfection, and luciferase activities were determined with a dual-luciferase reporter assay system and normalized for transfection efficiency, and the relative activities are shown when the values of mock cells were taken as 1.0. The experiment was performed in triplicate, and the values are the means ± SD (error bars). Statistical significance was evaluated by a two-tailed Dunnett's test and compared with the cells expressing Myc-PLEKHG1 alone: *$p < 0.1$; **$p < 0.01$. The data are shown as representative of three independent experiments. *B*, HEK293 cells were cotransfected with Myc-PLEKHG1WT and Flag-SRCWT, Flag-FYNWT, Flag-YES1WT, Flag-LCKWT, or Flag-LYNWT, as indicated. Cells were lysed 24 h after transfection, and immunoprecipitated with anti-Myc antibodies. Precipitated proteins were separated by SDS-PAGE and immunoblotted with anti-Myc antibody (for Myc-PLEKHG1WT) and anti-Flag antibody (for Flag-SRC, Flag-FYN, Flag-YES1, Flag-LCK, Flag-LYN). *C*, HEK293 cells were transfected with control Azami-Green, Flag-SRCWT or Flag-FYNWT, as indicated. Transfected cells were fixed and stained with Anti-Flag antibody, Acti-stain 555 conjugated Phalloidin and DAPI. Fluorescent images were observed by a confocal laser scanning microscope. The merged images show the Flag-tagged protein or mAG in *green*, phalloidin in *red* and DAPI in *blue*. Scale bar, 20 μm. *D*, HEK293 cells were cotransfected with mAG-PLEKHG1WT and Flag-SRCWT or Flag-FYNWT, as indicated. Transfected cells were fixed and stained with Acti-stain 555 conjugated Phalloidin and DAPI and observed by a confocal laser scanning microscope. The merged images show mAG in *green*, phalloidin in *red*, and DAPI in *blue*. Scale bar, 10 μm. *Arrowheads*, filopodia-like protrusions; *Arrows*, lamellipodia-like actin-rich protrusions. *E*, HEK293 cells were cotransfected with expression vectors for Myc-PLEKHG1WT and Flag-SRCWT or Flag-FYNWT. Transfected cells were lysed 24 h after transfection, the lysates were incubated with the bacterially produced GST-CRIB domain of PAK for 1 h, and the precipitation of GTP-bound forms of Cdc42 (active Cdc42) and Cdc42 was determined by immunoblotting. The data shown are representative of three independent experiments. *F*, quantitative analysis of the band intensity of GTP-Cdc42 from the pull-down assay of Figure 1*E*. The values of the quantification analysis were obtained from three independent experiments by dividing the band intensity of GTP-Cdc42 by the band intensity of Total-Cdc42 and are shown as the means ± SD (error bars). **$p < 0.01$. IB, immunoblotting; IP, immunoprecipitation; mAG, monomeric Azami green fluorescent protein; n.s., not significant; TCL, total cell lysate.

nucleotide exchange activity of PLEKHG1. Consistent with the results of SRF measurements, coexpression of Myc-PLEKHG1WT and Flag-FYNWT significantly increased the amount of active Cdc42 in HEK293 cells compared with the level by coexpression of Myc-PLEKHG1WT and Flag-SRCWT (Fig. 1, *E* and *F*). These results indicate that FYN signaling strongly activates PLEKHG1 compared with signaling by other SFKs.

These results suggest that the enhancement of PLEKHG1 RhoGEF activity and actin cytoskeleton rearrangement by FYN may be related to the tyrosine phosphorylation of PLEKHG1 and the interaction of PLEKHG1 with FYN.

Kinase activity is required for the regulation of PLEKHG1 activity by FYN

To examine whether FYN kinase activity is required for the enhancement of PLEKHG1 activity by FYN, we used an FYN mutant that has impaired kinase activity (FYNK299M), which was produced by substituting the lysine residue at amino acid 299 of FYN to a methionine. The results showed that the PLEKHG1-induced SRF-dependent gene transcriptional enhancement by FYN was significantly attenuated in cells coexpressing Myc-PLEKHG1WT and Flag-FYNK299M compared with cells coexpressing Myc-PLEKHG1WT and Flag-FYNWT (Fig. 2*A*). To evaluate the effect of FYN kinase activity on PLEKHG1-induced Cdc42 activation, we compared the intensity of Cdc42 activation in FYNWT-transfected cells and FYNK299M-transfected cells by GST-CRIB pull-down assays. The results showed that the amount of active Cdc42 in cells coexpressing Myc-PLEKHG1WT and Flag-FYNK299M was significantly lower than that in cells coexpressing Myc-PLEKHG1WT and Flag-FYNWT (Fig. 2, *B* and *C*). In addition, to investigate whether the FYNK299M mutant affects the tyrosine phosphorylation of PLEKHG1 and its interaction with PLEKHG1, immunoprecipitation experiments were performed using cells coexpressing Myc-PLEKHG1WT and either Flag-FYNK299M or Flag-FYNWT. The results showed that FYNK299M had less effect on the tyrosine phosphorylation of PLEKHG1 than did FYNWT, and the amount of Flag-FYNK299M coprecipitated with Myc-PLEKHG1WT was much less than the amount of Flag-FYNWT coprecipitated with Myc-PLEKHG1WT (Fig. 2*D*). These results demonstrated that the kinase activity of FYN is important for the interaction with PLEKHG1 and the enhancement of PLEKHG1 activity.

In general, carboxy-terminal Src kinase (CSK) is known to negatively regulate SFKs by phosphorylating the tyrosine residue located at the C-terminus (23). We therefore used CSK to examine whether the activation of FYN is required for PLEKHG1 activation. To investigate the effect of CSK on the interaction between PLEKHG1 and FYN, cells were coexpressed with Myc-PLEKHG1WT, Flag-FYNWT, and Myc-CSK, and then immunoprecipitation was performed using anti-Flag-tag antibody. We found that coprecipitation with Flag-FYNWT and Myc-PLEKHG1WT was not observed in cells coexpressing Flag-FYNWT, Myc-PLEKHG1WT, and

Myc-CSK (Fig. 2*E*). We also found that coprecipitation with Flag-FYNWT and Myc-CSK was not observed in the same cells. At this time, the tyrosine phosphorylation of PLEKHG1 was also attenuated in the cells coexpressing Flag-FYNWT, Myc-PLEKHG1WT, and Myc-CSK. Therefore, we examined the effect of CSK on the enhancement of PLEKHG1-induced SRF-dependent gene transcription by FYN. The results showed that FYN did not increase PLEKHG1-induced SRF-dependent gene transcription in cells coexpressing Myc-CSK (Fig. 2*F*). These results suggested that activation of FYN is required for the FYN-PLEKHG1-Cdc42 axis.

PLEKHG1 interacts with the N-terminal region containing the SH3 and SH2 domains of FYN

To investigate which regions of FYN interact with PLEKHG1, we prepared several Flag-tagged truncated mutants of FYN and performed immunoprecipitation experiments (Fig. 3*A*). As shown in Figure 3*B*, Myc-PLEKHG1 was coprecipitated with Flag-FYN 1–249 and Flag-FYN 81–249, which contains the SH3 and SH2 domains involved in the interaction of FYN with other proteins (24). Flag-FYN 141–249, which contains only the SH2 domain, was also coprecipitated weakly. In addition, Myc-PLEKHG1 was tyrosine-phosphorylated in cells coexpressing Myc-PLEKHG1 and Flag-FYN 1–249, Flag-FYN 81–249, or Flag-FYN 141–249. The band intensity of tyrosine-phosphorylated Myc-PLEKHG1 correlated with that of the coimmunoprecipitated FYN-fragments 1–249, 1–144, 141–249, and 81–249. Although the detailed mechanism is unknown, these tyrosine phosphorylations of Myc-PLEKHG1 may be related to the phosphorylation of PLEKHG1 by some endogenous kinase(s) expressed in HEK293 cells. This result suggested that the region of FYN containing the SH2 domain is required for the interaction with tyrosine-phosphorylated PLEKHG1. To further investigate whether these mutants affect PLEKHG1 activity, we measured the PLEKHG1-dependent gene transcription levels in cells coexpressing Myc-PLEKHG1 and various Flag-FYN mutants. As a result, the PLEKHG1-induced SRF-dependent gene transcription levels in cells coexpressing Myc-PLEKHG1 and Flag-FYN 1–249 increased, whereas there was almost no enhancement of the PLEKHG1-induced SRF-dependent gene transcription levels in cells coexpressing Myc-PLEKHG1WT and Flag-FYN 1–144, Flag-FYN 141–249, or Flag-FYN 81–249, respectively (Fig. 3*C*). These results suggested that the region of amino acids 1 to 249, which contains the SH4, SH3, and SH2 domains, in FYN is important for the interaction with PLEKHG1 and the enhancement of PLEKHG1 RhoGEF activity. To investigate whether tyrosine phosphorylation is required to enhance the interaction between FYN 1–249 and PLEKHG1WT, we performed immunoprecipitation assays in cells coexpressing PLEKHG1 and Flag-FYN 250–537, which has tyrosine kinase activity, and/or Flag-FYN 1–249, which lacks tyrosine kinase activity. As a result, the amount of FYN 1–249 coprecipitated with PLEKHG1WT appeared to be increased in cells coexpressing Myc-PLEKHG1WT, Flag-FYN 1–249, and Flag-FYN 250–537 compared with that in cells
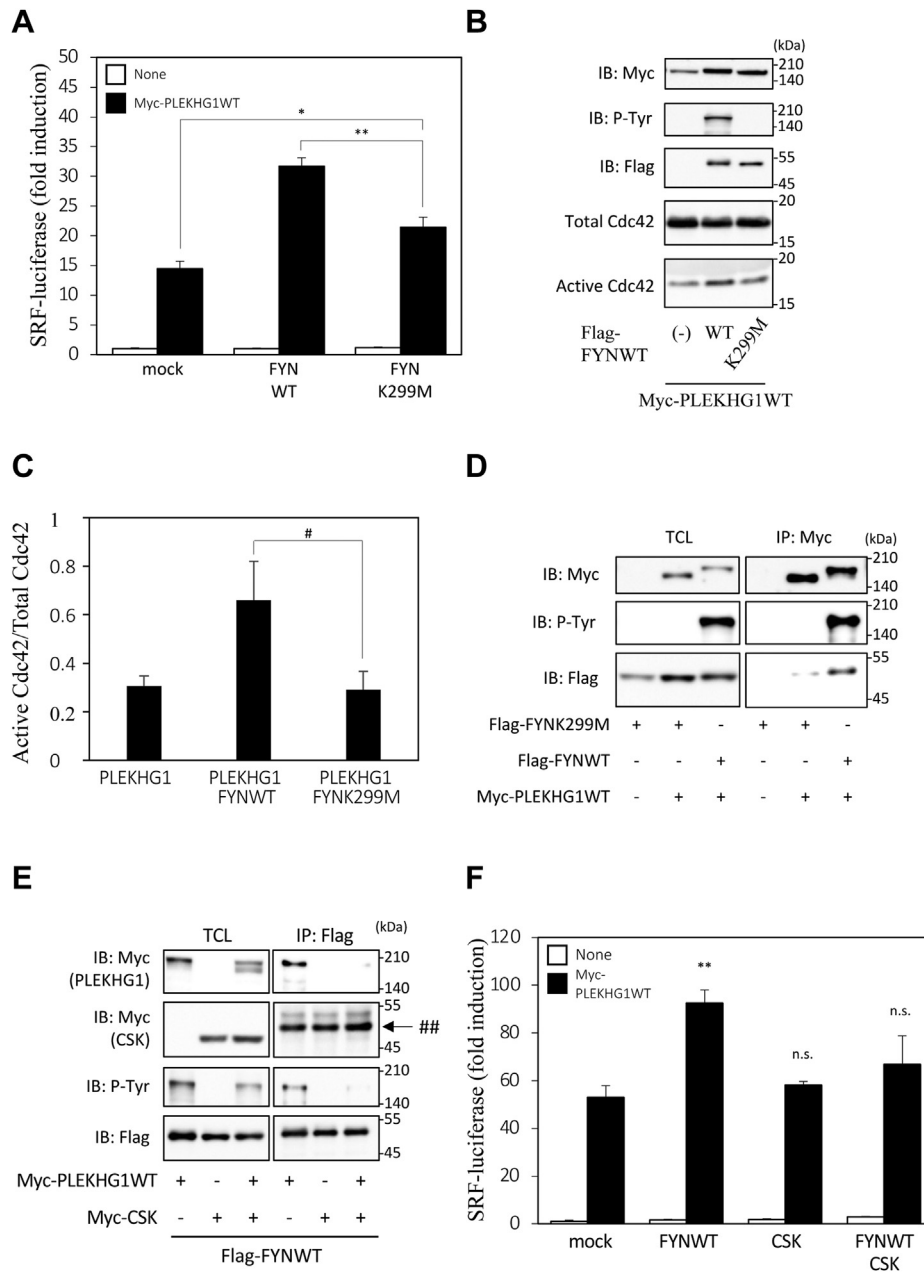
Figure 2. Kinase activity is required for the regulation of PLEKHG1 activity by FYN. *A*, HEK293 cells were cotransfected with pSRF.L-luciferase, pRL-SV40, and expression vectors for Myc-PLEKHG1 and Flag-FYNWT or Flag-FYNK299M, as indicated. Transfected cells were lysed 24 h after transfection, luciferase activities were determined with a dual-luciferase reporter assay system and normalized for transfection efficiency, and the relative activities are shown when the values of mock cells were taken as 1.0. The experiment was performed in triplicate, and the values are the means ± SD (error bars). Statistical significance was evaluated by two-tailed Tukey's test: *$p < 0.1$; **$p < 0.01$. The data are shown as representative of three independent experiments. *B*, HEK293 cells were cotransfected with expression vectors for Myc-PLEKHG1WT and Flag-FYNWT or Flag-FYNK299M as indicated. Transfected cells were lysed 24 h after transfection, the lysates were incubated with the bacterially produced GST-CRIB domain of PAK for 1 h, and the precipitation of GTP-bound forms of Cdc42 (Active Cdc42) and Cdc42 was determined by immunoblotting. The data shown are representative of three independent experiments. *C*, quantitative analysis of the band intensity of GTP-Cdc42 from the pull-down assay of Figure 2E. The values of the quantification analysis were obtained from three independent experiments by dividing the band intensity of GTP-Cdc42 by the band intensity of Total-Cdc42, and are shown as the means ± SD (error bars). #$p < 0.05$. *D*, HEK293 cells were cotransfected with Myc-PLEKHG1WT and Flag-FYNWT or Flag-FYNK299M, as indicated. Cells were lysed 24 h after transfection, and immunoprecipitated with anti-Myc antibodies. Precipitated proteins were separated by SDS-PAGE and immunoblotted with anti-Myc antibody (for Myc-PLEKHG1WT) and anti-Flag antibody (for Flag-FYNWT and Flag-FYNK299M). *E*, HEK293 cells were cotransfected with Myc-CSK, Myc-PLEKHG1WT, and Flag-FYNWT as indicated. Cells were lysed 24 h after transfection, and immunoprecipitated with anti-Flag antibodies. Precipitated proteins were separated by SDS-PAGE and immunoblotted with anti-Myc antibody (for Myc-PLEKHG1WT and Myc-CSK) and anti-Flag antibody (for Flag-FYNWT). ##nonspecific bands (*F*) HEK293 cells were cotransfected with pSRF.L-luciferase, pRL-SV40, and expression vectors for Myc-CSK, Myc-PLEKHG1WT and Flag-FYNWT, as indicated. Transfected cells were lysed 24 h after transfection, luciferase activities were determined with a dual-luciferase reporter assay system and normalized for transfection efficiency, and the relative activities are shown when the values of mock cells were taken as 1.0. The experiment was performed in triplicate, and the values are the means ± SD (error bars). Statistical significance was evaluated by a two-tailed Dunnett's test and compared with the cells expressing Myc-PLEKHG1 alone: *$p < 0.01$; **$p < 0.001$. The data are shown as representative of three independent experiments. IB, immunoblotting; IP, immunoprecipitation; n.s., not significant; TCL, total cell lysate.
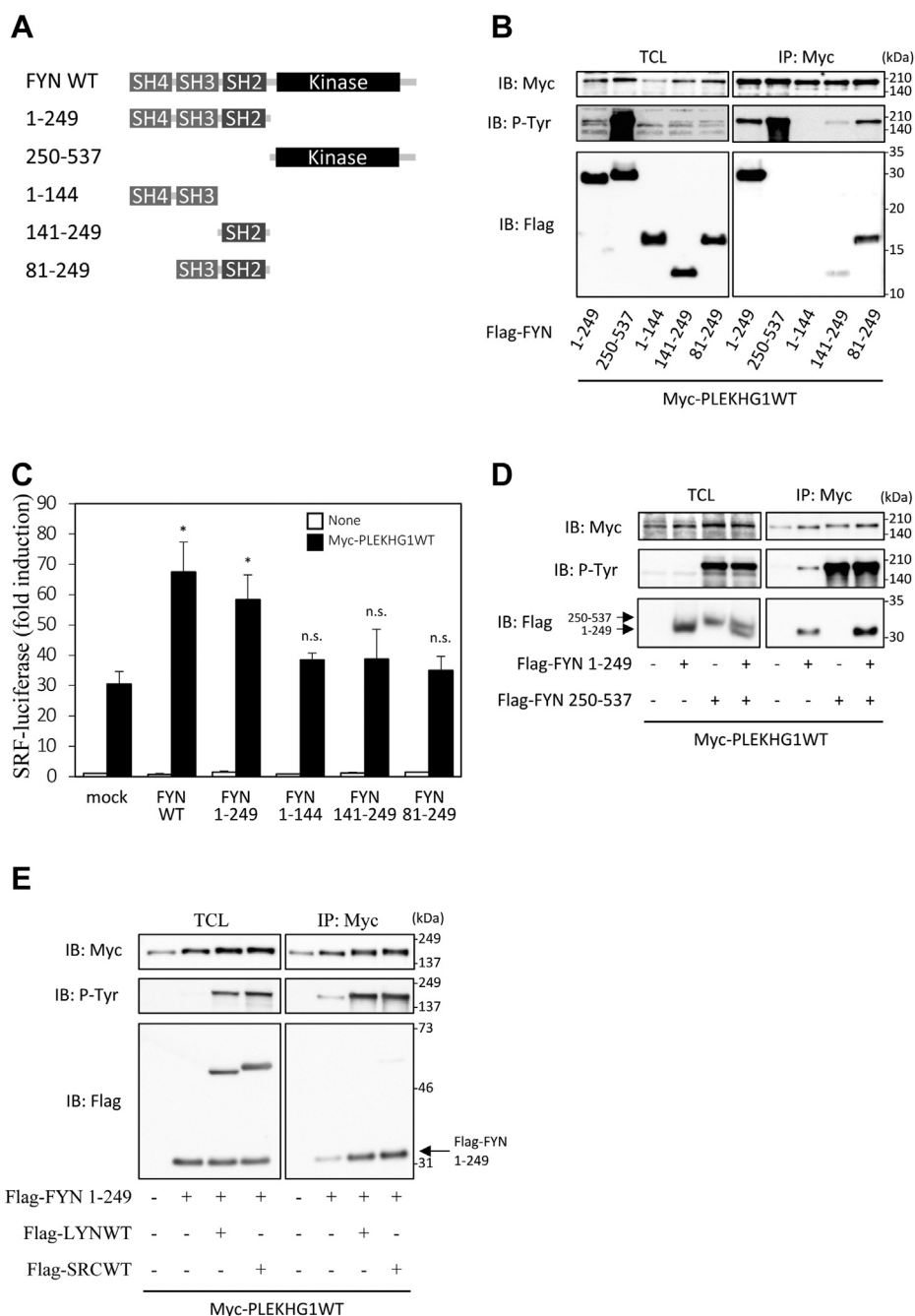
Figure 3. Identification of the PLEKHG1-interacting regions of FYN, and effects of the various FYN mutants on PLEKHG1-induced SRF-dependent gene transcription. *A*, structure of the proteins encoded by each expression plasmid: the WT, FYN 1–249, FYN 250–537, FYN 1–144, FYN 141–249, and FYN 81–249 constructs code for amino acid residues 1–249, 250–537, 1–144, 141–249, and 81–249 of FYN, respectively. *B*, HEK293 cells were cotransfected with Myc-PLEKHG1WT and Flag-FYNWT, Flag-FYN 1–249, Flag-FYN 250–537, Flag-FYN 1–144, Flag-FYN 141–249, or Flag-FYN 81–249 as indicated. Cells were lysed 24 h after transfection and immunoprecipitated with anti-Myc antibodies. Precipitated proteins were separated by SDS-PAGE and immunoblotted with anti-Myc antibody (for Myc-PLEKHG1WT) and anti-Flag antibody (for Flag-FYNWT and Flag-FYN mutants). *C*, HEK293 cells were co-transfected with pSRF.L-luciferase, pRL-SV40, and expression vectors for Myc-PLEKHG1WT and Flag-FYNWT, Flag-FYN 1–249, Flag-FYN 1–144, Flag-FYN 141–249, or Flag-FYN 81–249 as indicated. Transfected cells were lysed 24 h after transfection, the luciferase activities were determined with a dual-luciferase reporter assay system and normalized for transfection efficiency, and the relative activities are shown when the values of mock cells were taken as 1.0. The experiment was performed in triplicate, and the values are the means ± SD (error bars). Statistical significance was evaluated by a two-tailed Dunnett's test and compared with the cells expressing Myc-PLEKHG1 alone: n.s., not significant; *$p < 0.1$; **$p < 0.01$. The data are shown as representative of three independent experiments. *D*, HEK293 cells were cotransfected with Myc-PLEKHG1WT and Flag-FYN 1–249 or Flag-FYN 250–537 as indicated. Cells were lysed 24 h after transfection and immunoprecipitated with anti-Myc antibodies. Precipitated proteins were separated by SDS-PAGE and immunoblotted with anti-Myc antibody (for Myc-PLEKHG1WT) and anti-Flag antibody (for Flag-FYNWT and Flag-FYN mutants). *E*, HEK293 cells were cotransfected with Myc-PLEKHG1WT and Flag-FYN 1–249, Flag-LYNWT, or Flag-SRCWT as indicated. Cells were lysed 24 h after transfection and immunoprecipitated with anti-Myc antibodies. Precipitated proteins were separated by SDS-PAGE and immunoblotted with anti-Myc antibody (for Myc-PLEKHG1WT) and anti-Flag antibody (for Flag-FYN 1–249, Flag-LYNWT, and Flag-SRCWT). IB, immunoblotting; IP, immunoprecipitation; SH2, Src homology 2 domain; SH3, Src homology 3 domain; SH4, Src homology 4 domain; TCL, total cell lysate.

coexpressing PLEKHG1 and Flag-FYN 1–249 (Fig. 3D). At the same time, tyrosine phosphorylation of PLEKHG1 was also clearly increased by coexpression with Flag-FYN 250–537 (Fig. 3D). Therefore, to investigate whether other SFKs affect the interaction of PLEKHG1 with FYN 1–249, we used cells coexpressing Flag-FYN 1–249, Myc-PLEKHG1WT, and either Flag-LYNWT or Flag-SRCWT. As a result, we found that the level of tyrosine-phosphorylated PLEKHG1 and the amount of Flag-FYN 1–249 coprecipitated with Myc-PLEKHG1 was increased by cells coexpressing Flag-FYN 1–249, Myc-PLEKHG1WT, and either Flag-LYNWT or Flag-SRCWT. (Fig. 3E). These results suggest that not only FYN but also other SFK signals stabilize the interaction of PLEKHG1 with FYN 1–249 by phosphorylating PLEKHG1. Taken together, our data indicate that tyrosine phosphorylation of PLEKHG1 by FYN plays an important role in the interaction of PLEKHG1 with the SH4, SH3, and SH2 domain-containing regions of FYN and the activation of PLEKHG1 that occurs by these interactions.

The interaction of PLEKHG1 with FYN requires a region containing the phosphorylation sites of PLEKHG1

To investigate which regions of PLEKHG1 are required for binding to FYN, we generated various Myc epitope-tagged truncated mutants of PLEKHG1 as shown in Figure 4A and performed immunoprecipitation experiments. As shown in Figure 4B, Myc-PLEKHG1 553–1444 coprecipitated with Flag-FYNWT, whereas Myc-PLEKHG1 1–552 and Myc-PLEKHG1 862–1444 did not. Tyrosine phosphorylation of Myc-PLEKHG1 553–1444 but not Myc-PLEKHG1 1–552 or Myc-PLEKHG1 862–1444 could be detected at this time (Fig. 4B). We also examined the effects on PLEKHG1-induced SRF-dependent gene transcription by coexpression of Flag-FYNWT with Myc-PLEKHG1 1–552, which is thought to have RhoGEF activity due to the presence of the DH and PH domains. We confirmed that FYNWT itself has little effect on the SRF-dependent gene transcription. The level of SRF-dependent gene transcription in cells coexpressing Myc-PLEKHG1 and FYNWT was significantly increased compared with the level in cells expressing Myc-PLEKHG1. On the other hand, there was no difference between the level of SRF-dependent gene transcription in either cells coexpressing Myc-PLEKHG1 1–552 and FYNWT or cells expressing Myc-PLEKHG1 1–552. (Fig. 4C). These results suggest that the amino acid sequence from residues 553 to 861 of PLEKHG1 is essential for tyrosine phosphorylation and interaction with FYN. To elucidate the FYN interaction region of PLEKHG1 in detail, we generated several truncated mutants of PLEKHG1 and performed immunoprecipitation experiments. Tyrosine phosphorylation was detected in all of these Myc-PLEKHG1 truncated mutants, except for Myc-PLEKHG1 1–617. Myc-PLEKHG1 1–772, Myc-PLEKHG1 1–800, and Myc-PLEKHG1 1–856 showed particularly high levels of tyrosine phosphorylation (Fig. 4D). Coprecipitation of Flag-FYNWT with Myc-PLEKHG1 1–772, Myc-PLEKHG1 1–800, or Myc-PLEKHG1 1–856 was also observed at this time. The

amount of Flag-FYNWT coprecipitated with Myc-PLEKHG1 1–856 was clearly higher than the amounts coprecipitated with the other two mutants. We also examined the levels of SRF-dependent transcription in cells coexpressing these Myc-PLEKHG1 mutants and Flag-FYNWT. Consequently, we observed an enhancement of the levels of SRF-dependent gene transcription in cells coexpressing Flag-FYNWT and Myc-PLEKHG1WT and cells coexpressing Flag-FYNWT and Myc-PLEKHG1 1–856, but not in cells coexpressing Flag-FYNWT with other mutants (Fig. 4E). Therefore, to investigate whether PLEKHG1 1–856 interacts with FYN 1–249, we performed immunoprecipitation experiments in cells coexpressing Myc-PLEKHG1 1–856 and Flag-FYN 1–249. As a result, we found that FYN 1–249 interacted with PLEKHG1 1–856, but not with PLEKHG1 1–800 (Fig. 4F). Next, to investigate whether FYN interacts more directly with the interacting region of PLEKHG1, we prepared GST-fused PLEKHG1 553–862 and PLEKHG1 753–862 and used them to perform pull-down assays with Flag-FYNWT-expressing cell lysates. As a result, interactions of FYNWT with both the GST-fused PLEKHG1 553–862 and the GST-fused PLEKHG1 753–862 were detected. At this time, both GST-fused PLEKHG1 553–862 and GST-fused PLEKHHG1 753–862 were also tyrosine-phosphorylated during incubation with the cell lysate (Fig. 4G).

Activation of PLEKHG1 by FYN requires phosphorylation of multiple tyrosine residues

Our results so far suggest that the amino acid region 553–862 of PLEKHG1 plays an important role in the activation of PLEKHG1 by FYN *via* tyrosine phosphorylation and interaction. As shown in Figure 5A, there are six tyrosine residues in this amino acid region of PLEKHG1: Tyr-618, Tyr-720, Tyr-725, Tyr-773, Tyr-801, and Tyr-858. Using the Scansite 4 program, three tyrosine residues, Tyr-618, Tyr-720, and Tyr-801, were predicted to be the most likely to be phosphorylated among these tyrosine residues. To investigate how the phosphorylation of these tyrosines affects the activation of PLEKHG1 and its interaction with FYN, we generated PLEKHG1 mutants in which these three tyrosines were replaced with phenylalanine: Myc-PLEKHG1Y618F, Myc-PLEKHG1Y720F, Myc-PLEKHG1Y801F. In addition, we also produced Myc-PLEKHG1Y720,801F, a PLEKHG1 mutant in which both the Tyr-720 and Tyr-801 residues were replaced with phenylalanine, and Myc-PLEKHG1Y618,720,801F, a PLEKHG1 mutant in which all three of the Tyr-618, Tyr-720, and Tyr-801 residues were replaced with phenylalanine. As shown in Figure 5B, the tyrosine phosphorylation level of the PLEKHG1 mutant in cells coexpressing Flag-FYNWT with Myc-PLEKHG1Y720F or Myc-PLEKHG1Y801F was lower than that in cells coexpressing Flag-FYNWT with Myc-PLEKHG1WT or Myc-PLEKHG1Y618F. In addition, the tyrosine phosphorylation level of Myc-PLEKHG1Y720,801F in cells coexpressing Flag-FYNWT with Myc-PLEKHG1Y720,801F was further reduced in cells coexpressing Myc-PLEKHG1WT and Flag-FYNWT.
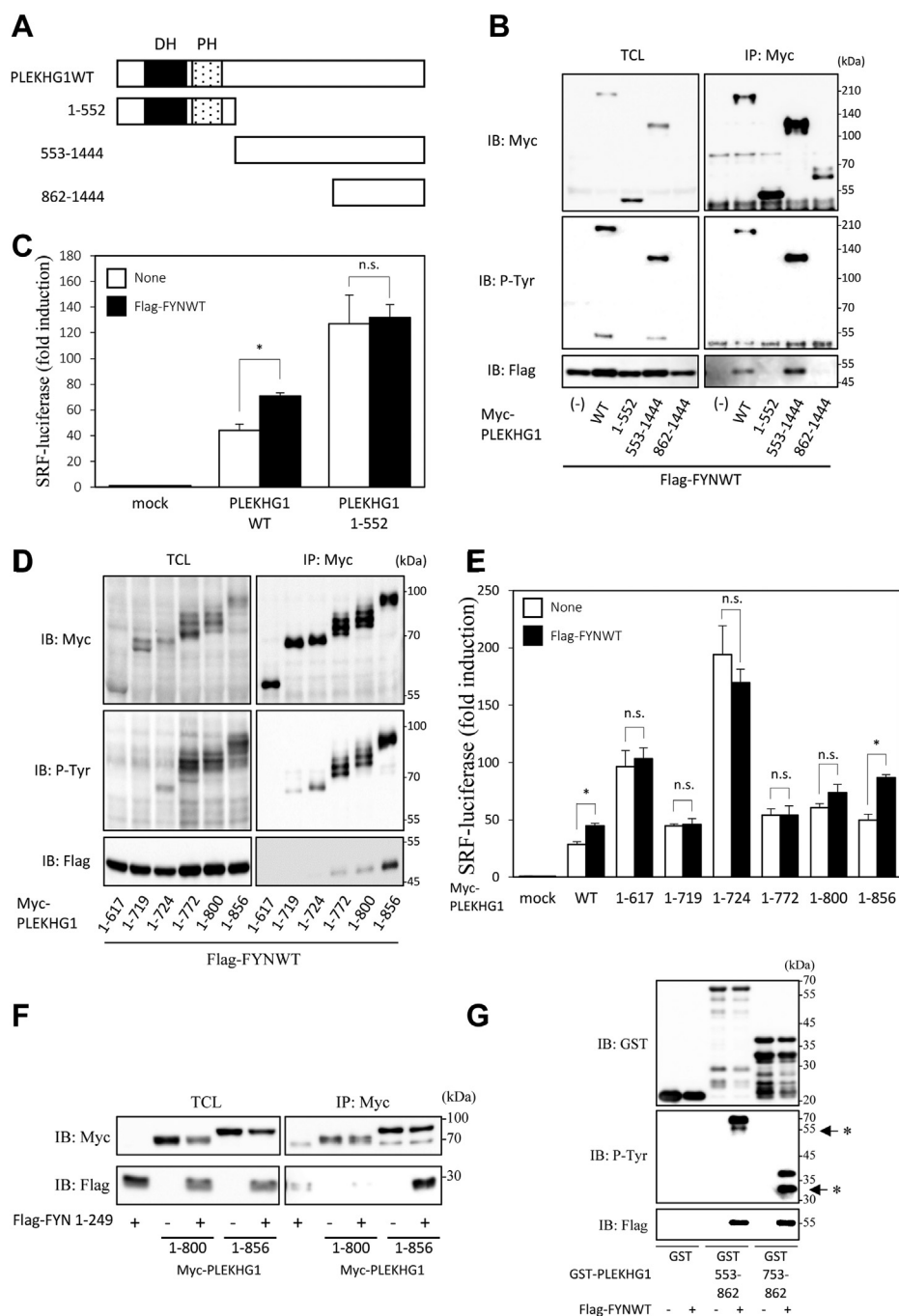
Figure 4. Identification of the FYN-interacting regions of PLEKHG1 and the effects of various PLEKHG1 mutants on SRF-dependent gene transcription. *A*, structure of the proteins encoded by each expression plasmid: the WT, PLEKHG1 1–552, FYN 553–1444, and FYN 862–1444 constructs code for amino acid residues 1–552, 553–1444, and 862–1444 of PLEKHG1, respectively. *B*, HEK293 cells were co-transfected with Myc-PLEKHG1WT, Myc-PLEKHG1 1–552, Myc-PLEKHG1 553–1444 or Myc-PLEKHG1 862–1444, and Flag-FYNWT as indicated. Cells were lysed 24 h after transfection and immunoprecipitated with anti-Myc antibodies. Precipitated proteins were separated by SDS-PAGE and immunoblotted with anti-Myc antibody (for Myc-PLEKHG1WT and Myc-PLEKHG1 mutants) and anti-Flag antibody (for Flag-FYNWT). *C*, HEK293 cells were cotransfected with pSRF.L-luciferase, pRL-SV40, and expression vectors for Myc-PLEKHG1WT, Myc-PLEKHG1 1–552, and Flag-FYNWT, as indicated. Transfected cells were lysed 24 h after transfection, the luciferase activities were determined with a dual-luciferase reporter assay system and normalized for transfection efficiency, and the relative activities are shown when the values of mock cells were taken as 1.0. The experiment was performed in triplicate, and the values are the means ± SD (error bars). Statistical significance was evaluated by a two-tailed unpaired Welch's *t* test: n.s., not significant; *$p < 0.01$; **$p < 0.001$. The data are shown as representative of three independent experiments. *D*, HEK293 cells were cotransfected with Myc-PLEKHG1WT, Myc-PLEKHG1 1–617, Myc-PLEKHG1 1–719, Myc-PLEKHG1 1–724, Myc-PLEKHG1 1–772, Myc-PLEKHG1 1–800 or Myc-PLEKHG1 1–856, and Flag-FYNWT as indicated. Cells were lysed 24 h after transfection and immunoprecipitated with anti-Myc antibodies. Precipitated proteins were separated by SDS-PAGE and immunoblotted with anti-Myc antibody (for Myc-PLEKHG1WT and Myc-PLEKHG1 mutants) and anti-Flag antibody (for Flag-FYNWT). *E*, HEK293 cells were cotransfected with Myc-PLEKHG1WT, Myc-PLEKHG1 1–617, Myc-PLEKHG1 1–719, Myc-PLEKHG1 1–724, Myc-PLEKHG1 1–772, Myc-PLEKHG1 1–800 or Myc-PLEKHG1 1–856, and Flag-FYN WT as indicated. Transfected cells were lysed 24 h after transfection, the luciferase activities were determined with a dual-luciferase reporter assay system and normalized for transfection efficiency, and the relative activities are shown when the values of mock cells were taken as 1.0. The experiment was performed in triplicate, and the values are the means ± SD (error bars). Statistical significance was evaluated by a two-tailed unpaired Welch's *t* test: *$p < 0.01$; **$p < 0.001$. The data are shown as representative of three independent experiments. *F*, HEK293 cells were cotransfected with Myc-PLEKHG1 1–800 or Myc-PLEKHG1 1–856, and Flag-FYN

At this time, the amount of Flag-FYNWT coimmunoprecipitated with anti-Myc antibody in cells coexpressing Flag-FYNWT and Myc-PLEKHG1Y720F or Myc-PLEKHG1Y801F were clearly lower than those in cells coexpressing Flag-FYNWT and Myc-PLEKHG1WT or Myc-PLEKHG1Y618. The amount of coimmunoprecipitated Flag-FYNWT was further reduced in cells coexpressing PLEKHG1Y720,801F and Flag-FYNWT (Fig. 5B). Moreover, the tyrosine phosphorylation level of Myc-PLEKHG1Y618,720,801F in cells coexpressing Flag-FYNWT with Myc-PLEKHG1Y618,720,801F was lower than that in cells coexpressing Flag-FYNWT with Myc-PLEKHG1WT. And the amount of coprecipitated Flag-FYNWT in cells coexpressing Myc-PLEKHG1Y618,720,801F and Flag-FYNWT was also reduced in cells coexpressing Myc-PLEKHG1WT and Flag-FYNWT (Fig. 5C). Next, we examined how tyrosine phosphorylation of PLEKHG1 affects the enhancement of PLEKHG1-induced SRF-dependent gene transcription levels by FYN, using these tyrosine-substitution mutants of PLEKHG1. We found a significant increase in SRF-dependent gene transcription levels by FYN in cells coexpressing Flag-FYNWT and Myc-PLEKHG1Y618F as well as in cells coexpressing Myc-PLEKHG1WT. Also, a significant SRF-dependent increase in gene transcription levels was observed in cells coexpressing Flag-FYNWT and Myc-PLEKHG1Y801F. On the other hand, there was no significant increase in the SRF-dependent gene transcription level in cells coexpressing Flag-FYNWT and either Myc-PLEKHG1Y720F, or Myc-PLEKHG1Y720,801F, or Myc-PLEKHG1Y618,720,801F (Fig. 5D). To examine whether tyrosine phosphorylation of PLEKHG1 by FYN affects the RhoGEF activity of PLEKHG1, we tested the activation of Cdc42 in cells coexpressing Myc-PLEKHG1Y618,720,801F and Flag-FYNWT by the pull-down assay using GST-CRIB. The results showed that the amount of active Cdc42 in cells coexpressing Myc-PLEKHG1Y618,720,801F and FYNWT was lower than that in cells coexpressing Myc-PLEKHG1WT and FYNWT (Fig. 5, E and F). Therefore, we examined whether the phosphorylation of Tyr-618, Tyr-720, and Tyr-801 in PLEKHG1 by FYN signaling affects cell morphology and actin cytoskeletal reorganization by using immunofluorescent staining and fluorescent phalloidin staining. It was confirmed that these mutations have little effect on the localization of PLEKHG1 and on the PLEKHG1-mediated morphological changes (*left* and *middle right* panels in Fig. 5G). FYN induced the PLEKHG1-mediated cell morphological changes (*middle left* panels in Fig. 5G), as described in Figure 1D. In contrast, there was no morphological difference between cells expressing Myc-PLEKHG1Y618,720,801F (*middle right* panels in Fig. 5G) and cells expressing Myc-PLEKHG1Y618,720,801F and Flag-FYNWT (*right* panels in Fig. 5G), suggesting that the tyrosine phosphorylation of PLEKHG1 by FYN induces actin cytoskeletal reorganization and regulates cell morphology. Taken together, these results suggest that the mechanism of PLEKHG1 activation by FYN involves the phosphorylation of multiple tyrosine residues, including at least Tyr-720 and Tyr-801, as well as the interaction of FYN with these phosphorylated tyrosine-containing regions and other regions in PLEKHG1. We assume that both the tyrosine phosphorylation and the interaction are important for the activation of PLEKHG1 by FYN.

Discussion

In this report, we provide evidence of a novel activation mechanism for PLEKHG1, a member of RhoGEFs, which involves the tyrosine phosphorylation by FYN and the interaction with FYN in HEK293 cells. The phosphorylation and the interaction are both related to PLEKHG1 activation each other. A previous study showed that phosphorylation at Tyr-2622 of Trio by FYN is essential for the proper assembly and stability of DCC/Trio signaling complexes at the cell surface of growth cones to mediate netrin-1-induced cortical axon outgrowth (6). We show that PLEKHG1 is phosphorylated by FYN signaling at multiple tyrosine residues. Although we do not currently know which of these phosphorylated tyrosine residues are most important for the PLEKHG1 activity, we have shown that the phosphorylation of two tyrosine residues, Tyr-720 and Tyr-801, is important for the regulation of GEF activity. Furthermore, phosphorylation of Tyr-720 and Tyr-801 in PLEKHG1 is required for the interaction between PLEKHG1 and FYN, and this interaction is also important for the regulation of PLEKHG1 activity in cells. We also present evidence that the phosphorylation of PLEKHG1 by FYN is regulated by CSK in cells. Therefore, we propose that PLEKHG1 is activated by FYN through phosphorylation of PLEKHG1 by FYN and interaction with FYN and induces an increase in SRF-dependent gene transcription and changes in cell morphology *via* activation of Rho signaling in cells that receive some stimulus that activates FYN (Fig. 6).

Our results demonstrate that the activation of PLEKHG1 requires an intact N-terminal region of FYN. In the coimmunoprecipitation analysis shown in Figure 3B, PLEKHG1 has a weaker interaction with FYN 81–249 than FYN 1–249. In addition, Figure 3C showed that FYN 81–249 has little effect on PLEKHG1-induced SRF-dependent gene transcription. The only structural difference between FYN 1–249 and FYN 81–249 is the presence of the SH4 domain, suggesting that the SH4 domain of FYN may play a role in increasing the SRF activity after the binding of PLEKHG1 to FYN. In general, the SH4 domain is thought to play an important role in determining the subcellular localization (of SFKs), including their translocation to the plasma membrane, by undergoing

---

1–249 as indicated. Cells were lysed 24 h after transfection and immunoprecipitated with anti-Myc antibodies. Precipitated proteins were separated by SDS-PAGE and immunoblotted with anti-Myc antibody (for Myc-PLEKHG1 mutants) and anti-Flag antibody (for Flag-FYN 1–249). G, Flag-FYNWT was incubated with GST, or GST-fused PLEKHG1 fragments 553–862 or 753–862. The protein complex was collected by glutathione-Sepharose, and the inclusion of Flag-FYNWT in the complexes was detected by immunoblotting. *These bands were thought to be degradation products of GST-PLEKHG1. DH, Dbl homology domain; IB, immunoblotting; IP, immunoprecipitation; n.s., not significant; PH, pleckstrin homology domain; TCL, total cell lysate.
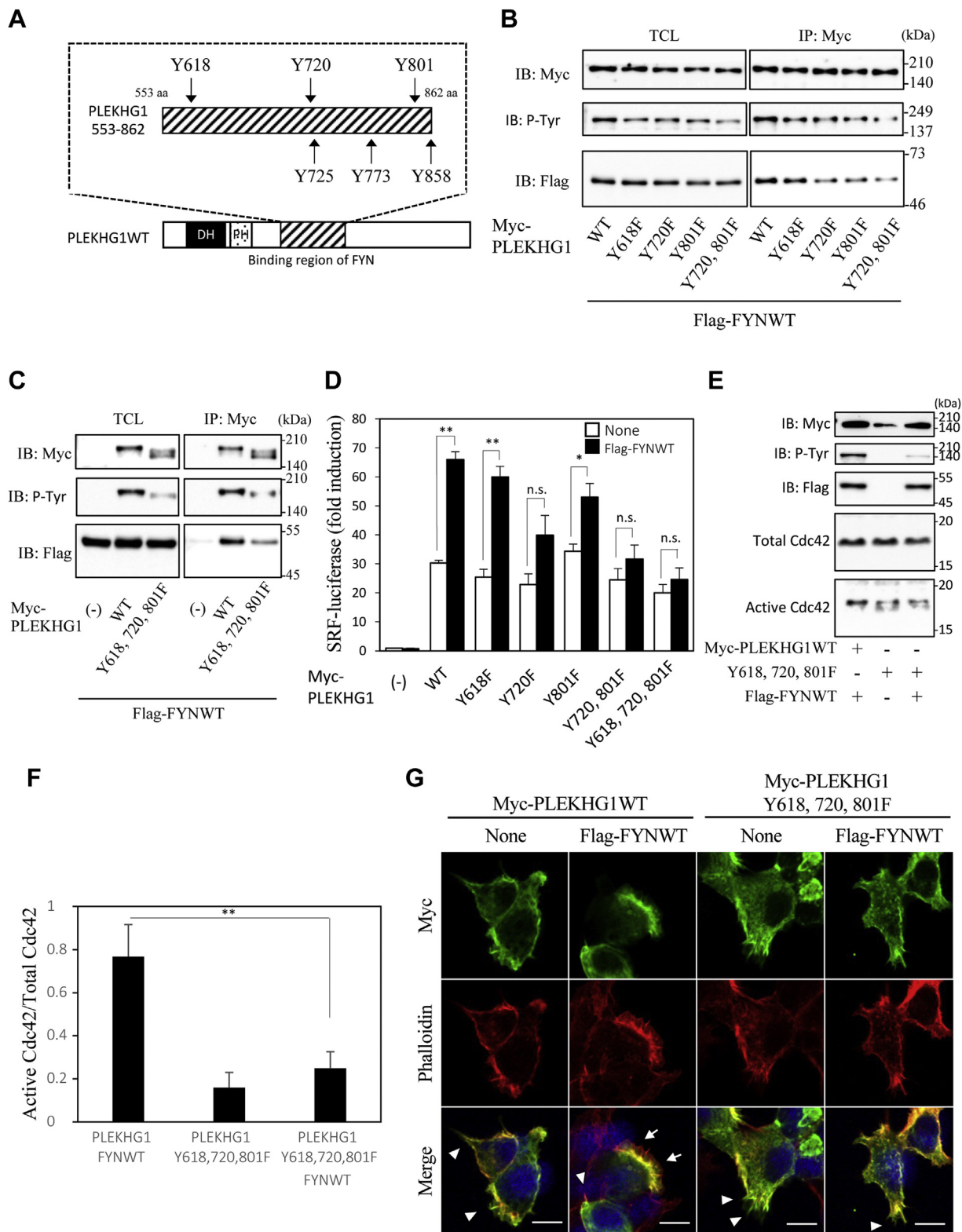
Figure 5. The importance of tyrosine phosphorylation of PLEKHG1 for the activation by and interaction with FYN. *A*, tyrosine residues on the PLEKHG1 amino acid region 553–862, which interacts with FYN: Tyr-618, Tyr-720, Tyr-725, Tyr-773, Tyr-801, and Tyr-858. *B*, HEK293 cells were cotransfected with Myc-PLEKHG1WT or Myc-PLEKHG1YF mutants (Y618F, Y720F, Y801F, and Y720,801F) and Flag-FYNWT as indicated. Cells were lysed 24 h after transfection, and immunoprecipitated with anti-Myc antibodies. Precipitated proteins were separated by SDS-PAGE and immunoblotted with anti-Myc antibody (for Myc-PLEKHG1WT and Myc-PLEKHG1YF mutants) and anti-Flag antibody (for Flag-FYNWT). *C*, HEK293 cells were cotransfected with Myc-PLEKHG1WT or Myc-PLEKHG1Y618,720,801F (Y618,720,801F) and Flag-FYNWT as indicated. Cells were lysed 24 h after transfection, and immunoprecipitated with anti-Myc antibodies. Precipitated proteins were separated by SDS-PAGE and immunoblotted with anti-Myc antibody (for Myc-PLEKHG1WT and Myc-PLEKHG1Y618,720,801F) and anti-Flag antibody (for Flag-FYNWT). *D*, HEK293 cells were co-transfected with pSRF.L-luciferase, pRL-SV40, and expression vectors for Myc-PLEKHG1YF mutants (Y618F, Y720F, Y801F, Y720,801F, and Y618,720,801F) and Flag-FYNWT, as indicated. Transfected cells were lysed 24 h
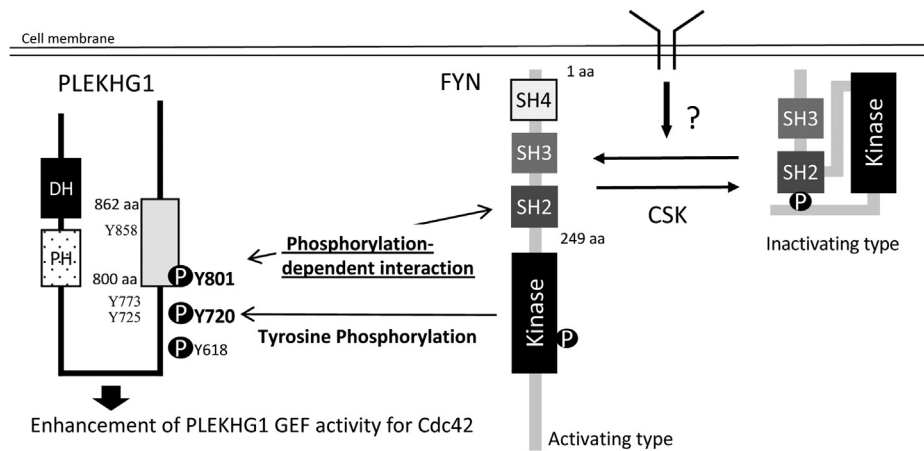
Figure 6. Schematic diagram of tyrosine phosphorylation of PLEKHG1 by FYN and the interaction between PLEKHG1 and FYN in the HEK293 cells. FYN is activated by receptor tyrosine kinases such as TNF-α and PDGF receptor (44, 45). However, in this study, we could not identify the physiological receptor that causes activation of Fyn and PLEKHG1. Activated FYN activates PLEKHG1 through phosphorylation of PLEKHG1 and interaction with PLEKHG1, thereby activating intracellular Cdc42 and enhancing SRF-dependent transcriptional activity. The activation of PLEKHG1 requires phosphorylation of Tyr-618, Tyr-720, and Tyr-801 in PLEKHG1 by FYN and the interaction of PLEKHG1 with FYN.

modifications induced by fatty acids such as palmitoylation and myristoylation (25–29). On the other hand, Cdc42, which is a partner for PLEKHG1, is also localized to the membrane by lipidation (1). Membrane localization of the complex of PLEKHG1 and FYN *via* the fatty-acid-modified SH4 domain of FYN could be required for FYN-PLEKHG1-Cdc42 signaling. Further analysis is needed to decide whether the SH4 domain is required for subcellular localization of the FYN and PLEKHG1 complex. We also show that both the SH3 and SH2 domains of FYN are required for interaction with PLEKHG1. It is generally known that the SH2 domain recognizes and binds to phosphorylated tyrosine in proteins, while the SH3 domain recognizes and binds to the PXXP motif in proteins (10, 11). We demonstrate that the interaction of PLEKHG1 with FYN mutants is only observed in the presence of a region containing the SH2 domain of FYN, and the SH3 domain of FYN alone is unable to interact with PLEKHG1 ([Fig. 3B](#)). This means that tyrosine phosphorylation of PLEKHG1 by the activation of intrinsic tyrosine kinases in cells is required for the interaction with SH2 domain of FYN.

Recently, it has been reported that FYN is required to promote ARHGEF16-induced proliferation and migration in colon cancer cells (30). It has also been reported that FYN binds to the N-terminal region of ARHGEF16, which contains five PXXP motifs to which the SH3 domain binds, and the SH3 domain of FYN is thought to bind to one of these PXXP motifs

(24). In contrast, the 800 to 862 amino acid region of PLEKHG1, to which the FYN binds, contains only one PXXP motif. Therefore, we created a mutant in which the proline of this PXXP motif was replaced by alanine and compared the interaction of the mutant with the FYN with PLEKHG1WT, but there was no significant difference (data not shown). Furthermore, we cannot confirm the interaction between the region containing only the SH3 domain of FYN and PLEKHG1. These results suggest that the SH3 domain is required for structural maintenance or for interaction with other molecules in the cell. Because PLEKHG1 has a large molecular weight and few known functional domains that have been structurally analyzed, we attempted to analyze PLEKHG1 by AlphaFold2, but could not obtain reliable results (31). However, structural analysis of the interaction between PLEKHG1 and FYN is considered to be very important. Further crystallographic studies of PLEKHG1 will provide more information about this complex.

PLEKHG1 has been reported as one of 11 RhoGEFs, including GEF-H1 (32) and Solo/ARHGEF40 (33), involved in cyclic stretch-induced reorientation in vascular endothelial cells (20). GEF-H1 was the first RhoGEF reported as a RhoGEF on cellular mechanoreception and has been reported as a RhoGEF for RhoA and Rac (34). LARG, another member of the RhoA-specific RhoGEFs, has also been reported as one of the RhoGEFs involved in mechanotransduction (35). It has

---

after transfection, the luciferase activities were determined with a dual-luciferase reporter assay system and normalized for transfection efficiency, and the relative activities are shown when the values of mock cells were taken as 1.0. The experiment was performed in triplicate, and the values are the means ± SD (error bars). Statistical significance was evaluated by a two-tailed unpaired Welch's *t* test: *$p < 0.01$; **$p < 0.001$. The data are shown as representative of three independent experiments. *E*, HEK293 cells were cotransfected with expression vectors for Myc-PLEKHG1WT or Myc-PLEKHG1Y618,720,801F, and Flag-FYNWT. Transfected cells were lysed 24 h after transfection, and lysates were incubated with the bacterially produced GST-CRIB domain of PAK for 1 h and the precipitation of GTP-bound forms of Cdc42 (Active Cdc42) and Cdc42 was determined by immunoblotting. The data shown are representative of three independent experiments. *F*, quantitative analysis of the band intensity of GTP-Cdc42 from the pull-down assay of [Figure 5E](#). The values of the quantification analysis were obtained from three independent experiments by dividing the band intensity of GTP-Cdc42 by the band intensity of Total-Cdc42, and are shown as the means ± SD (error bars). **$p < 0.01$. *G*, HEK293 cells were co-transfected with Myc-PLEKHG1WT or Myc-PLEKHG1Y618,720,801F, and Flag-FYNWT, as indicated. Transfected cells were fixed and stained with Acti-stain 555 conjugated Phalloidin and DAPI and observed by a confocal laser scanning microscope. The merged images show Myc in *green*, phalloidin in *red*, and DAPI in *blue*. Scale bar, 10 μm. *Arrowheads*, filopodia-like protrusions; *Arrows*, lamellipodia-like actin-rich protrusions. aa, amino acids; DH, Dbl homology domain; IB, immunoblotting; IP, immunoprecipitation; n.s., not significant; PH, pleckstrin homology domain; TCL, total cell lysate.

been reported that when stimulated by tension on cellular integrins, LARGs are activated by Fyn, whereas the catalytic activity of GEF-H1 is enhanced by ERKs downstream of a signaling cascade that includes FAK and Ras (35). Solo/ARHGEF40 is one of the RhoGEFs for RhoA and RhoC, and its keratin-binding capacity has recently been reported to be important for mechanotransduction (36). Furthermore, it has been reported that mechanical stretching in mesangial cells results in the activation of RhoA by VAV2 activation *via* the activation of SFKs and PI3-K (37). On the other hand, it has been reported that SFKs and p130Cas, one of the intracellular substrate molecules of SFKs, play an important role in cell reorientation upon cyclic stretch (38). It has also been reported that platelet endothelial cell adhesion molecule 1 (PECAM-1) is tyrosine-phosphorylated by Fyn in a flow- and stretch-dependent manner in vascular endothelial cells (39). These reports suggest that PLEKHG1 is phosphorylated through the activation of FYN *via* mechanotransduction from such as mechanical stimuli as cyclic stretch, and the resulting complex of FYN and PLEKHG1 may play some function in response to the morphological changes in cells expressing PLEKHG1. In the future, this point needs to be considered.

In summary, we demonstrate here for the first time that FYN, one of the five SFKs thought to be expressed in HEK293 cells, activates Cdc42 *via* activation of PLEKHG1, one of the RhoGEFs. We also propose that both tyrosine phosphorylation and interaction are important for the activation of PLEKHG1 by FYN. Since PLEKHG1 may be involved in various physiological functions and pathological conditions, further understanding of the activation mechanism of PLEKHG1 by FYN in different situations, such as mechanical stimulation (or disuse) and pathogenesis-related stress, may help us to understand various cellular functions.

Experimental procedures
Plasmids and reagents

The KIAA1209 cDNA clone, which was derived from a transcript from the PLEKHG1 gene, was used as the WT in this study. The PLEKHG1WT and the various deletion mutants of PLEKHG1 were subcloned into pF5K-CMV-neo-Myc or pIMR21-Myc vector by restriction enzyme digestion and polymerase chain reaction (PCR) amplification. The site-directed mutagenesis technique was used to substitute phenylalanine to create the various PLEKHG1YF mutants. The putative phosphotyrosine sites in PLEKHG1 were predicted by using Scansite 4 (https://scansite4.mit.edu/4.0). Scansite 4 predicts target motifs for different kinases using a positional selectivity matrix based on peptide library screening (40). It is known that searches using Scansite 4 apply a high level of stringency to identify the strongest motif matches. To prepare glutathione S-transferase (GST)-fused proteins, PLEKHG1 (553–862) and PLEKHG1 (753–862) were subcloned into pGEX-4T-1 vector by restriction enzyme digestion and ligation. Plasmids of the Src WT from Millipore and the full-length cDNA Fyn, Yes1, Lck, and Lyn were subcloned into the pF5A-CMV-neo-Flag vector by a Flexi system (Promega).

The various deletion mutants of FYN were subcloned into the pF5A-Flag vector by restriction enzyme digestion and PCR amplification. The site-directed mutagenesis technique was used to substitute methionine to generate the FYNK299M mutants. The pSRF.L-luciferase reporter plasmid was purchased from Stratagene, and pRL-SV40 was purchased from Nippon Gene. Mouse monoclonal antibodies against Myc-epitope and Flag-epitope were purchased from Wako Pure Chemical Industries. Antiphosphotyrosine antibody was purchased from Santa Cruz.

Cell culture and transfection

HEK293 (ATCC CRL 1573) cells were grown in DMEM supplemented with 10% FBS in a CO_2 (5%) incubator at 37 °C. Transient transfection was performed using Polyethylenimine Max (PolySciences Inc.) (41). Cells were transfected with DNA for 6 h and then washed with serum-free DMEM and incubated for 16 to 18 h in DMEM.

Dual-luciferase reporter gene assay

HEK293 cells seeded in 24-well plates were cotransfected with the indicated expression plasmids together with the pSRF.L luciferase reporter plasmids and the pRL-SV40 control reporter plasmids. After transfection, the cells were washed once with ice-cold PBS and lysed with passive lysis buffer. Luciferase activities were determined by using a Dual-Luciferase Reporter assay system (Promega). The activity of the reporter gene was normalized against the activity of the control vector. The experiment was performed in triplicate, and the values are the means ± SD (error bars). The data shown are representative of three independent experiments (42).

Immunoprecipitation

Transfected cells seeded in 6-cm dishes were washed once with ice-cold PBS and lysed with lysis buffer (50 mM Tris-HCl, pH 7.5, 100 mM NaCl, 0.1 mM EDTA, 1 mM Na_3VO_4, 0.5% Nonidet P-40, phosphatase inhibitor solution (Roche), and protease inhibitor solution (Roche)). The lysates were centrifuged to remove residue (16,100g for 10 min). Clear lysates were incubated with 1.0 μg of anti-Myc IgG or 1.0 μg of anti-Flag IgG for 2 h at 4 °C and then mixed with protein G-agarose beads (EMD Millipore Co) for 1 h at 4 °C. The beads were washed three times with washing buffer (50 mM Tris-HCl, pH 7.5, 100 mM NaCl, 0.1 mM EDTA, 1 mM Na_3VO_4, 0.1% Nonidet P-40, phosphatase inhibitor, and protease inhibitor solution), and the bound proteins were eluted with sample buffer. Equal amounts of samples were resolved by poly-acrylamide gel electrophoresis (SDS-PAGE). The transferred PVDF membranes were tested by immunoblot analysis. In brief, the membranes were blocked with PVDF Blocking Reagent for Can Get Signal (Toyobo Co). For the detection of Myc-tag and Flag-tag, we used HRP-conjugated mouse anti-Myc IgG (FUJIFILM Wako Pure Chemical Co) and mouse anti-Flag IgG (FUJIFILM Wako Pure Chemical Corp.), respectively. For the detection of P-Tyr, we used mouse anti-P-Tyr IgG (Santa Cruz). For the detection of these first

antibodies, we used HRP-conjugated anti-mouse IgG (MBL Co) and anti-rabbit IgG (MBL Co) as secondary antibodies. Visualization of HRP-labeled proteins was performed using enzyme-linked chemiluminescence (Thermo Fisher Scientific) and an LAS-4000 luminescent image analyzer (GE Healthcare).

Protein–protein interaction in vitro assay

GST, GST-PLEKHG1 553–862, and GST-PLEKHG1 753–862 were expressed and extracted from *E. coli* strain BL21 and bound to glutathione-Sepharose 4B. The purified GST fusion protein (with the glutathione-agarose beads) and cell lysate were incubated for 2 h at 4 °C in lysis buffer. Beads were washed three times with lysis buffer, and bound proteins were separated by SDS-PAGE and detected by immunoblotting using various antibodies (14).

Pull-down assays with PAK-CRIB beads for Cdc42 activation

Transfected cells seeded in 6-cm dishes were washed once with ice-cold PBS and lysed with lysis buffer (20 mM Tris-HCl, pH 7.5, 100 mM NaCl, 0.5% Nonidet P-40, 2 mM $MgCl_2$, and protease inhibitor solution (Roche)). The lysates were centrifuged to remove residue ($16,100{\times}g$ for 10 min). Bacterially produced GST–CRIB proteins bound to glutathione–Sepharose beads were incubated with the lysates for 1 h at 4 °C. The beads were then washed by lysis buffer, and the binding of Cdc42-GTP in the lysates to the CRIB domains was analyzed by SDS–PAGE and immunoblotting for Cdc42 (43). The experiment was performed at least three times. The values of the quantification analysis were obtained by dividing the band intensity of GTP-Cdc42 by the band intensity of Total-Cdc42 and are shown as the means ± SD (error bars). Band intensity was measured by using Image J software.

Immunoblot analysis

Transfected cells seeded in 24-well plates were washed once with ice-cold PBS and lysed with 1% (w/v) SDS in distilled water. The protein amount of each lysate was quantified using a bicinchoninic acid protein assay kit (Thermo Scientific), with BSA as the standard. The same amounts of protein were subjected to 7.5% SDS-PAGE. The transferred PVDF membrane was blocked by PVDF Blocking Reagent for Can Get Signal (Toyobo). For the detection of Myc-tag, FLAG-tag, and phosphotyrosine, we used mouse anti-Myc antibody, mouse anti-FLAG antibody, and anti-phosphotyrosine antibody, respectively. To detect Myc-tag and Flag-tag, we used HRP-conjugated anti-mouse IgG as a secondary antibody (MBL Co). Visualization of HRP-labeled proteins was performed using enzyme-linked chemiluminescence detection reagents (GE Healthcare or PerkinElmer Life Science) and an LAS-4000 luminescent image analyzer (GE Healthcare).

Immunofluorescent analysis

Transfected cells cultured on coverslips were washed once with ice-cold PBS and fixed with 4% formaldehyde for 30 min. Fixed cells were permeabilized with 0.1% Triton X-100 in PBS and washed four times with PBS. Then, the cells were blocked with 10% goat serum in PBS for 1 h. Cells were washed with PBS and incubated with the indicated primary antibodies and subsequently with secondary antibodies labeled with Alexa Fluor 488 (Thermo Fisher Scientific). F-actin was visualized using Acti-stain 555 phalloidin and the nuclei were visualized using Cellstain DAPI solution (DOJINDO). The coverslips were then mounted with Fluoromount (Diagnostic Bio-Systems). Labeled cells were analyzed by using a Zeiss laser scanning confocal microscope (LSM-710; Carl Zeiss).

Data availability

All data relating to this manuscript are contained in the manuscript.

Conflict of interest—The authors declare that they have no conflict of interest with the contents of this article. All authors consented to participate, read the manuscript, and gave consent for publication. All data and materials are available for publication. No authors have competing interests.

Abbreviations—The abbreviations used are: DH, Dbl homology; PH, pleckstrin homology; Rho, Rho family small GTPases; RhoGEFs, Rho-specific guanine nucleotide exchange factor; SFK, Src family tyrosine kinase; SH, src homology; SRF, serum response factors.

References

1. Hodge, R. G., and Ridley, A. J. (2016) Regulating Rho GTPases and their regulators. *Nat. Rev. Mol. Cell Biol.* **17**, 496–510
2. Rossman, K. L., Der, C. J., and Sondek, J. (2005) GEF means go: Turning on Rho GTPases with guanine nucleotide-exchange factors. *Nat. Rev. Mol. Cell Biol.* **6**, 167–180
3. Schmidt, A., and Hall, A. (2002) Guanine nucleotide exchange factors for Rho GTPases: Turning on the switch. *Genes Dev.* **16**, 1587–1609
4. Itoh, R. E., Kiyokawa, E., Aoki, K., Nishioka, T., Akiyama, T., and Matsuda, M. (2008) Phosphorylation and activation of the Rac1 and Cdc42 GEF Asef in A431 cells stimulated by EGF. *J Cell Sci.* **121**, 2635–2642
5. Feng, Q., Baird, D., Yoo, S., Antonyak, M., and Cerione, R. A. (2010) Phosphorylation of the cool-1/β-pix protein serves as a regulatory signal for the migration and invasive activity of Src-transformed cells. *J. Biol. Chem.* **285**, 18806–18816
6. DeGeer, J., Boudeau, J., Schmidt, S., Bedford, F., Lamarche-Vane, N., and Debant, A. (2013) Tyrosine phosphorylation of the Rho guanine nucleotide exchange factor trio regulates netrin-1/DCC-mediated cortical axon outgrowth. *Mol. Cell. Biol.* **33**, 739–751

7. Nakano, S., Nishikawa, M., Asaoka, R., Ishikawa, N., Ohwaki, C., Sato, K., Nagaoka, H., Yamakawa, H., Nagase, T., and Ueda, H. (2019) DBS is activated by EPHB2/SRC signaling-mediated tyrosine phosphorylation in HEK293 cells. *Mol. Cell. Biochem.* **459**, 83–93

8. Manning, G., Whyte, D. B., Martinez, R., Hunter, T., and Sudarsanam, S. (2002) The protein kinase complement of the human genome. *Science* **298**, 1912–1934

9. Lowell, C. A., and Soriano, P. (1996) Knockouts of Src-family kinases: Stiff bones, wimpy T cells, and bad memories. *Genes Dev.* **10**, 1845–1857

10. Thomas, S. M., and Brugge, J. S. (1997) Cellular functions regulated by Src family kinases. *Annu. Rev. Cell Dev. Biol.* **13**, 513–609

11. Brown, M. T., and Cooper, J. A. (1996) Regulation, substrates and functions of Src. *Biochim. Biophys. Acta* **1287**, 121–149

12. Frame, M. C. (2002) Src in cancer: Deregulation and consequences for cell behaviour. *Biochim. Biophys. Acta Rev. Cancer* **1602**, 114–130

13. Schiller, M. R., Chakrabarti, K., King, G. F., Schiller, N. I., Eipper, B. A., and Maciejewski, M. W. (2006) Regulation of RhoGEF activity by intramolecular and intermolecular SH3 domain interactions. *J. Biol. Chem.* **281**, 18774–18786

14. Sato, K., Suzuki, T., Yamaguchi, Y., Kitade, Y., Nagase, T., and Ueda, H. (2014) PLEKHG2/FLJ00018, a Rho family-specific guanine nucleotide exchange factor, is tyrosine phosphorylated via the EphB2/cSrc signaling pathway. *Cell. Signal.* **26**, 691–696

15. Nishikawa, M., Nakano, S., Nakao, H., Sato, K., Sugiyama, T., Akao, Y., Nagaoka, H., Yamakawa, H., Nagase, T., and Ueda, H. (2019) The interaction between PLEKHG2 and ABL1 suppresses cell growth via the NF-κB signaling pathway in HEK293 cells. *Cell. Signal.* **61**, 93–107

16. Franceschini, N., Fox, E., Zhang, Z., Edwards, T. L., Nalls, M. A., Sung, Y. J., Tayo, B. O., Sun, Y. V., Gottesman, O., Adeyemo, A., Johnson, A. D., Young, J. H., Rice, K., Duan, Q., Chen, F., *et al.* (2013) Genome-wide association analysis of blood-pressure traits in african-ancestry individuals reveals common associated genes in African and Non-African populations. *Am. J. Hum. Genet.* **93**, 545–554

17. Hunter, Z. R., Xu, L., Yang, G., Zhou, Y., Liu, X., Cao, Y., Manning, R. J., Tripsas, C., Patterson, C. J., Sheehy, P., and Treon, S. P. (2014) The genomic landscape of Waldenström macroglobulinemia is characterized by highly recurring MYD88 and WHIM-like CXCR4 mutations, and small somatic deletions associated with B-cell lymphomagenesis. *Blood* **123**, 1637–1646

18. Gray, K. J., Kovacheva, V. P., Mirzakhani, H., Bjonnes, A. C., Almoguera, B., DeWan, A. T., Triche, E. W., Saftlas, A. F., Hoh, J., Bodian, D. L., Klein, E., Huddleston, K. C., Ingles, S. A., Lockwood, C. J., Hakonarson, H., *et al.* (2018) Gene-centric analysis of preeclampsia identifies maternal association at PLEKHG1. *Hypertension* **72**, 408–416

19. Traylor, M., Tozer, D. J., Croall, I. D., Lisiecka Ford, D. M., Olorunda, A. O., Boncoraglio, G., Dichgans, M., Lemmens, R., Rosand, J., Rost, N. S., Rothwell, P. M., Sudlow, C. L. M., Thijs, V., Rutten-Jacobs, L., and Markus, H. S. (2019) Genetic variation in PLEKHG1 is associated with white matter hyperintensities (n = 11,226). *Neurology* **92**, E749–E757

20. Abiko, H., Fujiwara, S., Ohashi, K., Hiatari, R., Mashiko, T., Sakamoto, N., Sato, M., and Mizuno, K. (2015) Rho guanine nucleotide exchange factors involved in cyclic-stretch-induced reorientation of vascular endothelial cells. *J. Cell Sci.* **128**, 1683–1695

21. Reinhard, N. R., Van Der Niet, S., Chertkova, A., Postma, M., Hordijk, P. L., Gadella, T. W. J., and Goedhart, J. (2019) Identification of guanine nucleotide exchange factors that increase Cdc42 activity in primary human endothelial cells. *Small GTPases* **12**, 1–15

22. Hill, C. S., Wynne, J., and Treisman, R. (1995) The Rho family GTPases RhoA, Racl, and CDC42Hs regulate transcriptional activation by SRF. *Cell* **81**, 1159–1170

23. Sabe, H., Knudsen, B., Okada, M., Nada, S., Nakagawa, H., and Hanafusa, H. (1992) Molecular cloning and expression of chicken C-terminal Src kinase: Lack of stable association with c-Src protein. *Proc. Natl. Acad. Sci. U. S. A.* **89**, 2190–2194

24. Reebye, V., Frilling, A., Hajitou, A., Nicholls, J. P., Habib, N. A., and Mintz, P. J. (2012) A perspective on non-catalytic Src homology (SH) adaptor signalling proteins. *Cell. Signal.* **24**, 388–392

25. Wolven, A., Okamura, H., Rosenblatt, Y., and Resh, M. D. (1997) Palmitoylation of p59(fyn) is reversible and sufficient for plasma membrane association. *Mol. Biol. Cell* **8**, 1159–1173

26. Liang, X., Lu, Y., Wilkes, M., Neubert, T. A., and Resh, M. D. (2004) The N-terminal SH4 region of the Src family kinase Fyn is modified by methylation and heterogeneous fatty acylation: Role in membrane targeting, cell adhesion, and spreading. *J. Biol. Chem.* **279**, 8133–8139

27. Tournaviti, S., Hannemann, S., Terjung, S., Kitzing, T. M., Stegmayer, C., Ritzerfeld, J., Walther, P., Grosse, R., Nickel, W., and Fackler, O. T. (2007) SH4-domain-induced plasma membrane dynamization promotes bleb-associated cell motility. *J. Cell Sci.* **120**, 3820–3829

28. Sato, I., Obata, Y., Kasahara, K., Nakayama, Y., Fukumoto, Y., Yamasaki, T., Yokoyama, K. K., Saito, T., and Yamaguchi, N. (2009) Differential trafficking of Src, Lyn, Yes and Fyn is specified by the state of palmitoylation in the SH4 domain. *J. Cell Sci.* **122**, 965–975

29. Yeo, M. G., Oh, H. J., Cho, H. S., Chun, J. S., Marcantonio, E. E., and Song, W. K. (2011) Phosphorylation of Ser 21 in Fyn regulates its kinase activity, focal adhesion targeting, and is required for cell migration. *J. Cell. Physiol.* **226**, 236–247

30. Yu, B., Xu, L., Chen, L., Wang, Y., Jiang, H., Wang, Y., Yan, Y., Luo, S., and Zhai, Z. (2020) FYN is required for ARHGEF16 to promote proliferation and migration in colon cancer cells. *Cell Death Dis.* **11**, 1–14

31. Jumper, J., Evans, R., Pritzel, A., Green, T., Figurnov, M., Ronneberger, O., Tunyasuvunakool, K., Bates, R., Žídek, A., Potapenko, A., Bridgland, A., Meyer, C., Kohl, S. A. A., Ballard, A. J., Cowie, A., *et al.* (2021) Highly accurate protein structure prediction with AlphaFold. *Nature* **596**, 583–589

32. Ren, Y., Li, R., Zheng, Y., and Busch, H. (1998) Cloning and characterization of GEF-H1, a microtubule-associated guanine nucleotide exchange factor for Rac and Rho GTPases. *J. Biol. Chem.* **273**, 34954–34960

33. Tse, S. W., Broderick, J. A., Wei, M. L., Luo, M. H., Smith, D., McCaffery, P., Stamm, S., and Andreadis, A. (2005) Identification, expression analysis, genomic organization and cellular location of a novel protein with a RhoGEF domain. *Gene* **359**, 63–72

34. Birukova, A. A., Fu, P., Xing, J., Yakubov, B., Cokic, I., and Birukov, K. G. (2010) Mechanotransduction by GEF-H1 as a novel mechanism of ventilator-induced vascular endothelial permeability. *Am. J. Physiol. Lung Cell. Mol. Physiol.* **298**, L837–L848

35. Guilluy, C., Swaminathan, V., Garcia-Mata, R., O'Brien, E. T., Superfine, R., and Burridge, K. (2011) The Rho GEFs LARG and GEF-H1 regulate the mechanical response to force on integrins. *Nat. Cell Biol.* **13**, 722–728

36. Fujiwara, S., Matsui, T. S., Ohashi, K., Mizuno, K., and Deguchi, S. (2019) Keratin-binding ability of the N-terminal Solo domain of Solo is critical for its function in cellular mechanotransduction. *Genes Cells* **24**, 390–402

37. Peng, F., Zhang, B., Ingram, A. J., Gao, B., Zhang, Y., and Krepinsky, J. C. (2010) Mechanical stretch-induced RhoA activation is mediated by the RhoGEF Vav2 in mesangial cells. *Cell. Signal.* **22**, 34–40

38. Niediek, V., Born, S., Hampe, N., Kirchgeßner, N., Merkel, R., and Hoffmann, B. (2012) Cyclic stretch induces reorientation of cells in a Src family kinase- and p130Cas-dependent manner. *Eur. J. Cell Biol.* **91**, 118–128

39. Chiu, Y. J., McBeath, E., and Fujiwara, K. (2008) Mechanotransduction in an extracted cell model: Fyn drives stretch- and flow-elicited PECAM-1 phosphorylation. *J. Cell Biol.* **182**, 753–763

40. Obenauer, J. C., Cantley, L. C., and Yaffe, M. B. (2003) Scansite 2.0: Proteome-wide prediction of cell signalling interactions using short sequence motifs. *Nucleic Acids Res.* **31**, 3635–3641

41. Godbey, W. T., Wu, K. K., and Mikos, A. G. (1999) Poly(ethylenimine) and its role in gene delivery. *J. Control Release* **60**, 149–160

42. Ueda, H., Nagae, R., Kozawa, M., Morishita, R., Kimura, S., Nagase, T., Ohara, O., Yoshida, S., and Asano, T. (2008) Heterotrimeric G protein βγ subunits stimulate FLJ00018, a guanine nucleotide exchange factor for Rac1 and Cdc42. *J. Biol. Chem.* **283**, 1946–1953

43. Sander, E. E., Van Delft, S., Ten Klooster, J. P., Reid, T., Van Der Kammen, R. A., Michiels, F., and Collard, J. G. (1998) Matrix-dependent

Tiam1/Rac signaling in epithelial cells promotes either cell-cell adhesion or cell migration and is regulated by phosphatidylinositol 3-kinase. *J. Cell Biol.* **143**, 1385–1398

44. Angelini, D. J., Hyun, S. W., Grigoryev, D. N., Garg, P., Gong, P., Singh, I. S., Passaniti, A., Hasday, J. D., and Goldblum, S. E. (2006) TNF-α increases tyrosine phosphorylation of vascular endothelial cadherin and opens the paracellular pathway through fyn activation in human lung endothelia. *Am. J. Physiol. Lung Cell. Mol. Physiol.* **291**, L1232–L1245

45. Hansen, K., Alonso, G., Courtneidge, S. A., Ronnstrand, L., and Heldin, C. H. (2006) PDGF-induced phosphorylation of Tyr28 in the N-terminus of fyn affects fyn activation. *Biochem. Biophys. Res. Commun.* **241**, 355–362